

190. A Mesoscale Analysis of the Development of Storms and Transition to Supercells during the Indiana and Ohio Tornado Outbreak of 24 August 2016

JEFFREY FRAME* AND KEVIN GRAY

Department of Atmospheric Sciences, University of Illinois at Urbana-Champaign, Urbana, IL

1. Introduction and motivation

On 24 August 2016, a tornado outbreak struck portions of Indiana and Ohio, producing 24 confirmed tornadoes, 6 of which were rated EF-2 or stronger on the Enhanced Fujita Scale (NCDC 2016; Fig. 1). During this outbreak, disorganized elevated convection developed into three discrete surface-based supercell thunderstorms from south to north. Shortly after each supercell organized, it produced a significant tornado (see cities in bold font in Fig. 1). This outbreak was also notable in that it was relatively unexpected. For example, neither Indiana nor Ohio was included in the 2% Tornado Risk area in the Storm Prediction Center Day 1 Convective Outlook issued at 1630 UTC, just hours before the first tornado occurred (Fig. 2).

Through a mesoscale analysis of surface, satellite, and radar observations, we identify several mesoscale features pertinent to this outbreak and that likely contributed to its low predictability. These features include two clusters of elevated storms over Illinois on the morning of the outbreak, an outflow boundary that was traced back to storms that occurred the previous evening over Nebraska and Iowa, a mesoscale convective vortex (MCV) that developed within these nocturnal storms, and a differential heating boundary that formed over Illinois and Indiana on the morning of the outbreak and persisted into the afternoon. In the next section, we discuss the overnight convection and outflow boundary and then discuss the transition to surface-based supercells in section 3. The tornadoes are discussed in section 4, and section 5 presents our conclusions.

2. Nocturnal convection and outflow boundary

During the evening of 23 August, a bowing thunderstorm complex organized over eastern Nebraska, which moved into southwestern Iowa by 0508 UTC (Fig. 3a). These storms produced a well-defined outflow boundary, as evidenced by the northwesterly wind sustained at 30 knots and gusting to 48 knots at Shenandoah, IA (south-

westernmost station in Iowa; Fig. 3b). Owing to radiative cooling of the near-surface air ahead of these storms, the temperature change across the gust front was only a few °F.

Using a combination of WSR-88D and surface observations, we tracked this outflow boundary as it moved eastward across Iowa at a calculated speed of 14.5 m s^{-1} through 0908 UTC (Fig. 4). By this time, the bow echo had dissipated and the outflow boundary was oriented along an approximate north-south line west of Iowa City and Cedar Rapids. In response to modest lower tropospheric warm advection (not shown), numerous elevated thunderstorms formed over eastern Iowa ahead of the outflow boundary between 0800 and 0900 UTC (Fig. 4a). We were unable to definitively track the outflow boundary after this time owing to limited low-level WSR-88D coverage between the KDMX and KDVN radars and the lack of a significant wind shift or temperature drop in the surface observations owing to the elevated convection.

By 1408 UTC, the widespread elevated convection that formed over eastern Iowa had consolidated into a small cluster of storms near Champaign, IL, on the southern end of a larger area of rain over northeastern Illinois (Fig. 5a). Visible satellite imagery reveals an arc of clouds over northwestern Illinois with approximately the same shape as the outflow boundary from the night before (Fig. 6) that was co-located with a slight surface wind shift from south-southwesterly winds ahead of the boundary to west-southwesterly winds behind it (Fig. 5b). The position of this wind shift was within 20 km of the estimated position of the outflow boundary using the speed calculated above. A few elevated storms had formed along this boundary north of Bloomington, IL. Extensive cloud cover from the leading cluster of storms resulted in a differential heating boundary extending southeastward across eastern Illinois from the suspected outflow boundary (Figs. 5b and 6). The differential heating boundary separated air that was 5-10°F cooler with south-southeasterly surface winds to its north from the south-southwesterly winds to its south (Fig. 5b). The MCV was near the Illinois/Iowa border at this time. Most convection-allowing model guidance initialized at 1200 UTC depicted one or both of these storm clusters

*Corresponding author address: Jeffrey Frame, Department of Atmospheric Sciences, University of Illinois at Urbana-Champaign, 1301 W. Green St., Urbana, IL, 61801; e-mail: frame@illinois.edu

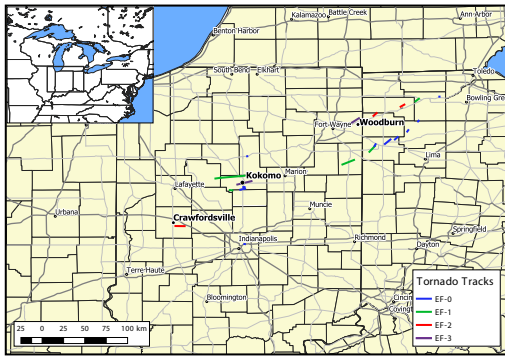


FIG. 1. Tornado tracks from 24 August 2016. Colors indicate the Enhanced Fujita Scale rating. Towns nearest the three significant tornadoes in Indiana are in bold text.

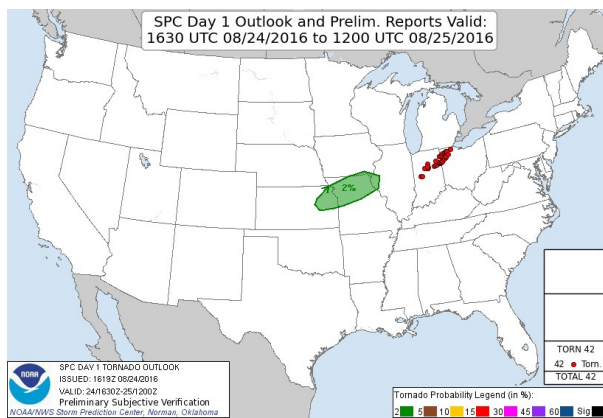


FIG. 2. Tornado probabilities from the SPC Day 1 Convective Outlook issued at 1630 UTC 24 August 2016. Red dots are preliminary tornado reports.

growing upscale and eventually becoming surface based across Indiana that afternoon, but generally did not exhibit supercellular convection in this region (not shown).

3. Transition to surface-based supercells

Over the next three hours, the leading cluster of storms dissipated over central Indiana, while the old outflow boundary and its associated storms continued to advance eastward to near the Illinois/Indiana state line (Fig. 7). The moist surface air did not permit significant evaporative cooling beneath the storms and stunted cold pool formation. Surface observations confirm that there was no strong outflow surging away from any storms through

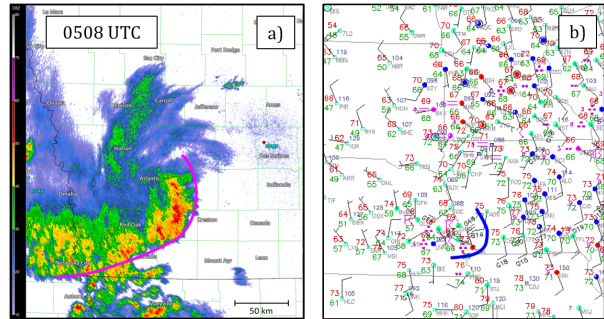


FIG. 3. (a) KDMX WSR-88D radar reflectivity and (b) surface station plot at 0508 UTC 24 August. Pink (a) or blue (b) line indicates the outflow boundary.

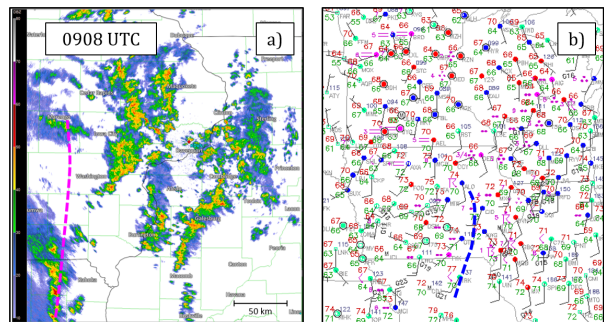


FIG. 4. (a) KDVN WSR-88D radar reflectivity and (b) surface station plot at 0908 UTC 24 August. Pink (a) or blue (b) line indicates the outflow boundary.

this time. In the succeeding four hours, three discrete surface-based tornadic supercells developed from this disorganized line of elevated convection, which is quite unusual.

There are several studies documenting how supercells or isolated convection grow into mesoscale convective systems (e.g., Bluestein and Weisman 2000; Finley et al. 2001; Dial et al. 2010), but a survey of the literature reveals the analysis of only one case in which a line or cluster of storms developed into supercells hours after initiation (Burgess and Curran 1985). On 26 April 1984, a line of storms transitioned into discrete tornadic supercells over central Oklahoma after dark. This transition was attributed to an increase in low-level storm-relative helicity (SRH) owing to the onset of the nocturnal low-level jet, while warm advection just above the surface reestablished the capping inversion. This likely permitted only rotating updrafts to survive because their associated upward-directed perturbation pressure gradient accelerations (e.g., Rotunno and Klemp 1982) can make

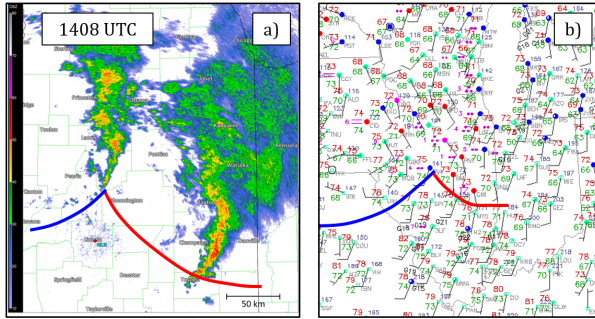


FIG. 5. (a) KILX WSR-88D radar reflectivity and (b) surface station plot at 1408 UTC 24 August. Blue line indicates the outflow boundary and red line indicates the differential heating boundary.

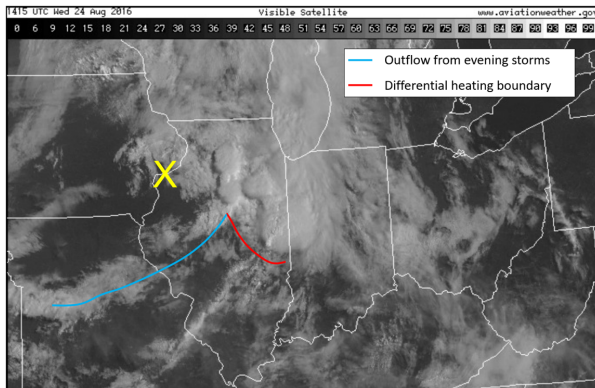


FIG. 6. Visible satellite image at 1415 UTC 24 August. Blue line indicates the outflow boundary, red line indicates the differential heating boundary, and yellow “X” indicates the MCV.

supercells less susceptible to deleterious environmental changes. On 24 August 2016, however, the transition to supercells occurred during the day in concert with diurnal destabilization; it is likely that the lack of a strong cold pool with the initially elevated storms allowed such a transition to occur.

The 1200 UTC sounding from Lincoln, IL, depicts a moist environment with strong shear in the lowest few hundred meters above ground level (AGL), with little shear above this (Fig. 8). By 1800 UTC, the environment across Indiana supported supercellular convection, and even tornadoes if a supercellular storm mode existed. The 0-1 km SRH was greater than $150 \text{ m}^2 \text{ s}^{-2}$ along and north of the differential heating boundary (Fig. 9a), while 0-6 km bulk shear values were between 30 and 40 knots on the southern flank of the MCV (Fig. 9b). Strong solar

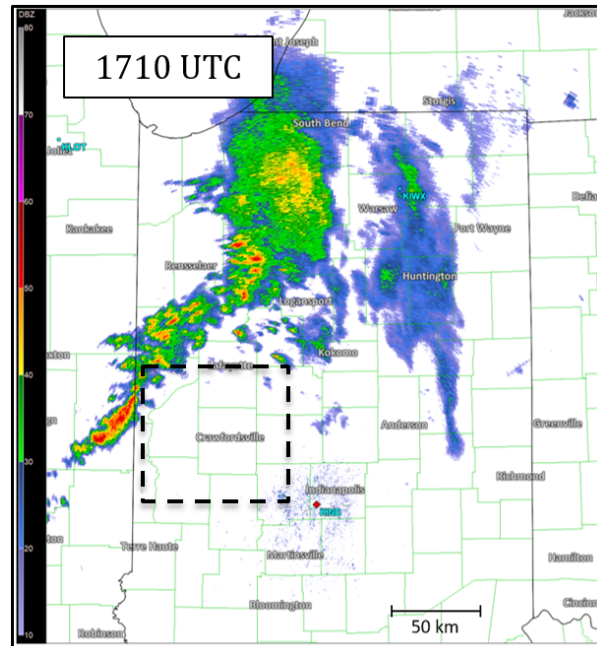


FIG. 7. KIND WSR-88D radar reflectivity at 1710 UTC 24 August. Black box indicates the zoomed in area in Figs. 10-12.

heating boosted mixed-layer CAPE to greater than 2000 J kg^{-1} along and south of the differential heating boundary and ahead of the old outflow boundary (Fig. 9c) amid a moist environment with lifting condensation level heights less than 1000 m (Fig. 9d).

The storm on the southern end of the remaining cluster gradually increased in size and intensity through 1758 UTC (Fig. 10a) as new updrafts formed south of it and merged with it. The storm still appeared multicellular, with several reflectivity maxima and only weak transient rotation (Fig. 10b). The lack of any sharp reflectivity gradients within this storm also suggests that the updrafts were relatively weak. By 1821 UTC, a strong updraft had developed on the southern flank of this cluster, with a sharp gradient and slight appendage in reflectivity collocated with convergence in radial velocity (Fig. 11). By 1834 UTC, 13 minutes later, the radial velocity field indicated strong rotation just south of a hook echo (Fig. 12). Several small cells south of this supercell continued to develop and merge with it, and as one such merger was ongoing at 1838 UTC, the supercell produced an EF-2 tornado near Crawfordsville, IN, that lasted for 10 minutes.

This transition from elevated to surface-based convection is consistent with that in a WRF simulation of this event (Gray and Frame 2018). In the simulation, initially elevated updrafts ingest more highly-sheared air from

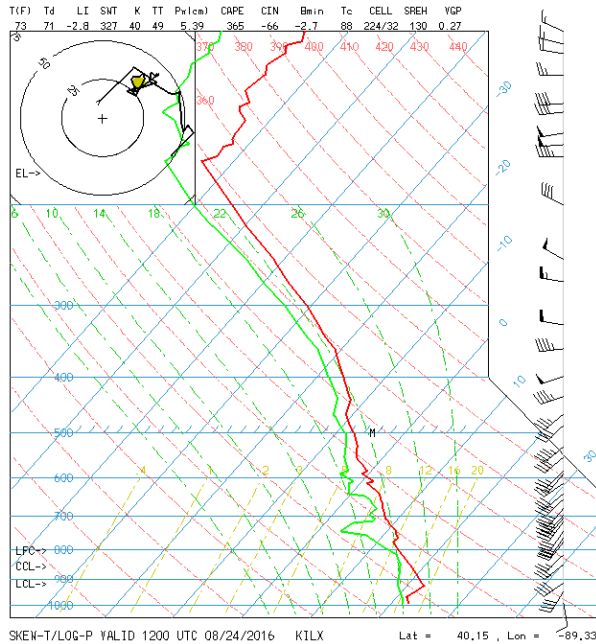


FIG. 8. Skew- T log- p diagram depicting the 1200 UTC 24 August sounding from Lincoln, IL (KILX).

near the surface, resulting in the development of stronger rotation and upward-directed perturbation pressure gradient forces, allowing the updrafts to ingest even more surface air and develop even stronger rotation. Given the environment in place (Fig. 8), any storm would have needed to be rooted near the surface for strong rotation to form since nearly all of the vertical wind shear was below 950 mb (roughly 300 m AGL). Storms that were rooted above this layer ingested very little effective bulk shear as the winds were southwesterly between 30 and 40 knots from 950 to 500 mb.

4. Production of tornadoes

As discussed above, the first surface-based supercell to form from the initially elevated convective cluster produced an EF-2 tornado near Crawfordsville, IN, at 1838 UTC. Radar imagery while this storm was organizing depicts that it was on the southern end of an otherwise disorganized line of storms (Fig. 13a). The old outflow boundary from the convection the previous evening was analyzed along this line of storms, and it intersected the differential heating boundary near where this supercell developed and ultimately produced its first tornado (Fig. 13b).

The second supercell to form developed similarly to the first, originating from convective pulses in the thin line of storms that stretched from Logansport to near Lafayette at 1810 UTC (Fig. 13a). It became a super-

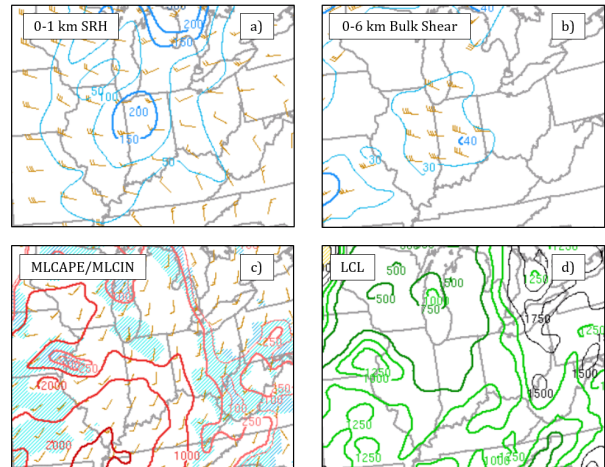


FIG. 9. (a) 0-1 km storm relative helicity ($\text{m}^2 \text{s}^{-2}$), (b) 0-6 km bulk wind shear (knots), (c) mixed-layer CAPE (J kg^{-1} ; contoured) and CIN ($> 25 \text{ J kg}^{-1}$ shaded), and (d) lifting condensation level height (m).

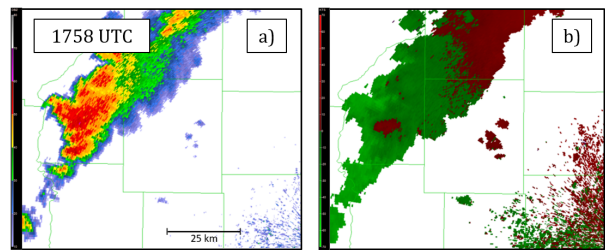


FIG. 10. KIND WSR-88D (a) radar reflectivity and (b) radial velocity (knots) at 1758 UTC 24 August.

cell by 1907 UTC near Kokomo (Fig. 14a). The differential heating boundary moved northward during this period and was also in the vicinity of Kokomo (Fig. 14b). Shortly after the time of this image, at 1920 UTC, this supercell produced an EF-3 tornado that caused damage in Kokomo.

Two hours later, around 2100 UTC, a third supercell developed near Fort Wayne from updraft pulses within the broad region of lighter precipitation over northeastern Indiana (Figs. 14a and 15a). This supercell produced an EF-3 tornado near the town of Woodburn, in far eastern Indiana, at 2127 UTC. This storm would go on to produce several more tornadoes in northwestern Ohio, including three that were rated EF-2 (Fig. 1). The supercells that produced the tornadoes near Kokomo and Crawfordsville continued moving eastward; although these storms produced additional tornadoes, they were all rated EF-1 or weaker. A second round of supercells

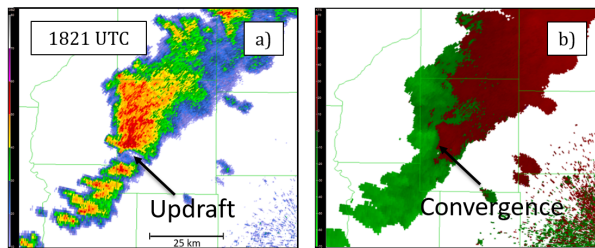


FIG. 11. As in Fig. 10 only at 1821 UTC.

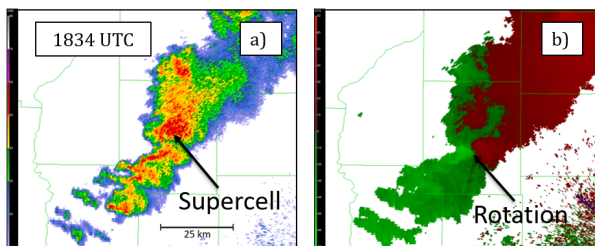


FIG. 12. As in Fig. 10 only at 1834 UTC.

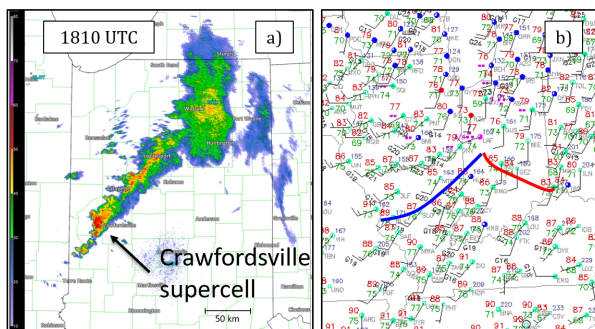


FIG. 13. As in Fig. 5 only at 1810 UTC.

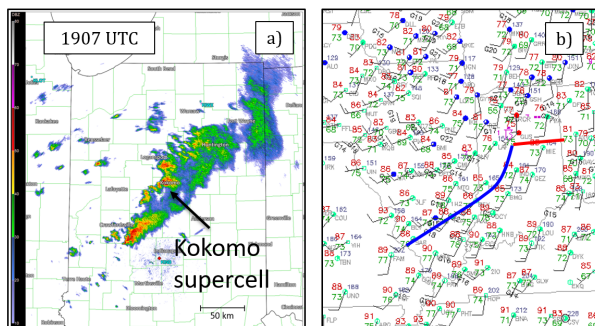


FIG. 14. As in Fig. 5 only at 1907 UTC.

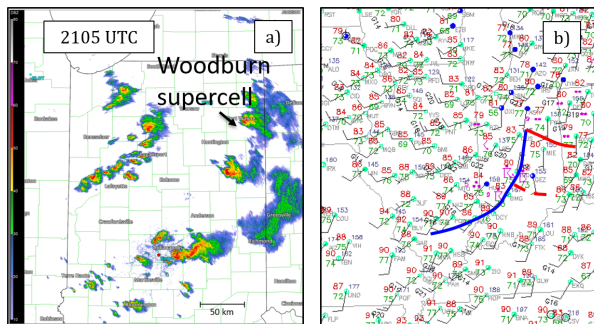


FIG. 15. As in Fig. 5 only at 2105 UTC.

formed over north-central Indiana and some of these storms produced tornadoes as well, including a second tornado near Kokomo (Fig. 1). The 2100 UTC surface analysis reveals that the differential heating boundary had moved northward and was just south of Fort Wayne, while a secondary differential heating boundary formed owing to extensive cloud cover associated with the other two supercells farther south (Fig. 15b).

The differential heating boundary between the cloud-shaded region to its north and relatively clear skies to its south appears to have been instrumental in the production of significant tornadoes during this outbreak, all of which occurred in close proximity to the differential heating boundary (Fig. 16).¹ A companion WRF simulation (Gray and Frame 2018) reveals that reduced vertical mixing beneath the cloud cover north of the differential heating boundary preserved vertical wind shear, and thus SRH there, while stronger mixing in regions that experienced more sun allowed southwesterly momentum to mix downward from aloft, reducing the vertical shear and SRH. These results are consistent with those of Frame and Markowski (2010, 2013) who noted modulations to the near-surface vertical wind shear beneath the anvils of simulated supercell thunderstorms.

5. Conclusions

On 24 August 2016, 24 tornadoes, including 6 significant tornadoes, struck Indiana and Ohio during a surprise outbreak. All of the significant tornadoes were produced by three supercells that devolved from initially disorganized elevated convection that formed that morning over Illinois along an outflow boundary from storms the previous evening. Additionally, an MCV from these nocturnal storms enhanced lower tropospheric wind fields on its southern flank, resulting in sufficient vertical wind shear

¹According to *Storm Data*, the westernmost significant tornado track in Ohio is actually two separate tornado tracks. The endpoint of the first tornado is so close to the beginning point of the second that these appear as a single tornado track in Fig. 16.

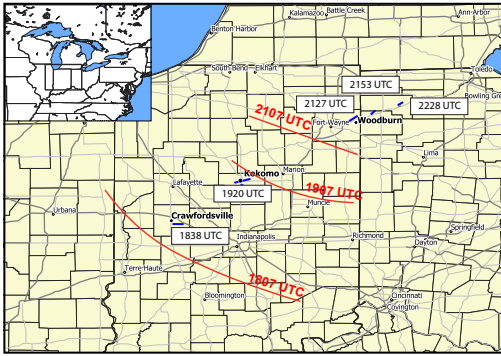


FIG. 16. Significant tornado tracks from 24 August 2016. The time each tornado began is listed in the white boxes. Red lines indicate the approximate locations of the differential heating boundary, as determined from satellite and surface observations. Towns nearest the three significant tornadoes in Indiana are in bold text.

for supercell and tornado formation. Nearly all of the shear, however, was confined within the lowest few hundred meters AGL, meaning that storms could not develop into supercells until they began ingesting highly-sheared near-surface air. Solar heating gradually destabilized the environment ahead of these storms and as updraft pulses accessed this strongly-sheared air, they began rotating.

The supercells formed from south to north across central Indiana, coinciding with the northward movement of a differential heating boundary. Cloud cover north of this boundary reduced solar heating and led to less vigorous vertical mixing, permitting stronger near-surface shear to exist than in regions in full sun south of the boundary. All six significant tornadoes in this outbreak occurred in close proximity to this differential heating boundary.

Much of the convection-allowing model output from the morning of 24 August depicted the initial elevated storms developing into a surface-based line and racing across Indiana that afternoon (not shown), possibly because the models produced too much or too cold outflow, allowing for the transition into an outflow-dominant linear mode. Instead, the initial multicellular convection did not produce strong, surging outflow, permitting a transition to discrete supercells once the storms became surface based. A correct forecast of this event would also have required an accurate simulation of the MCV, which augmented the vertical wind shear, the remnant outflow boundary, which triggered the initial storms, and the differential heating boundary, for reasons discussed above. Since most of these are subtle mesoscale features, the existence of which depends on antecedent or ongoing con-

vection, it is easy to see why this was such a challenging forecast.

Acknowledgments. The authors are grateful to the Department of Atmospheric Sciences at the University of Illinois for financial support. Radar figures were produced using GR2Analyst and tornado track figures were produced using QGIS. We are also grateful to discussions with Roger Edwards (SPC) and Brian Curran (NWS Midland/Odessa, TX) which helped inspire and improve this work.

REFERENCES

- Bluestein, H. B., and M. L. Weisman, 2000: The interaction of numerically-simulated supercells initiated along lines. *Mon. Wea. Rev.*, **128**, 3138-3149.
- Burgess, D. W., and E. B. Curran, 1985: The relationship of storm type to environment in Oklahoma on 26 April 1984. *Preprints, 14th Conf. on Severe Local Storms*, Indianapolis, IN, Amer. Meteor. Soc., 208-211
- Dial, G. L., J. P. Racy, and R. L. Thompson, 2010: Short-term convective mode evolution along synoptic boundaries. *Wea. Forecasting*, **25**, 1430-1446.
- Finley, C. A., W. R. Cotton, and R. A. Pielke, Sr., 2001: Numerical simulation of tornadogenesis in a high-precipitation supercell. Part I: Storm evolution and transition into a bow echo. *J. Atmos. Sci.*, **58**, 1597-1629.
- Frame, J. W., and P. M. Markowski, 2010: Numerical simulations of radiative cooling beneath the anvils of supercell thunderstorms. *Mon. Wea. Rev.*, **138**, 3024-3047.
- Frame, J. W., and P. M. Markowski, 2013: Dynamical influences of anvil shading on simulated supercell thunderstorms. *Mon. Wea. Rev.*, **141**, 2802-2820.
- Gray, K. T., and J. W. Frame, 2018: Investigating the transition from elevated multicellular convection to surface-based supercells as observed in the Indiana and Ohio tornado outbreak of 24 August 2016 using a WRF model simulation and perturbation pressure decomposition. *29th Conf. on Severe Local Storms*, Stowe, VT, Amer. Meteor. Soc.
- NCDC, 2016: *Storm Data*. Vol. 58, No. 8, 533 pp. [Available from National Climatic Data Center, 151 Patton Ave., Asheville, NC, 28801-5001.]
- Rotunno, R. and J. B. Klemp, 1982: The influence of the shear-induced pressure gradient on thunderstorm motion. *Mon. Wea. Rev.*, **110**, 136-151.